Advanced BLDC Motor Drive for Low Cost and High Performance Propulsion System in Electric and Hybrid Vehicles

B. K. Lee, *Student Member, IEEE* and M. Ehsani, *Fellow, IEEE*

Texas A&M University, Dept. of Electrical Engineering
College Station, TX 77843-3128, U.S.A
Tel: 979-845-7582, Fax: 979-862-1976

Abstract-**In this paper, we propose an advanced brushless dc motor (BLDCM) drive for low cost and high performance electric propulsion system in electric vehicles (EV's) and hybrid electric vehicles (HEV's). It includes reduced parts power converter topologies and an optimal PWM control strategy to produce the desired dynamic and static speed and torque characteristics. The theoretical explanation and operational principle are described in detail. And, the performance of the proposed low cost BLDCM drive is compared with the conventional counterpart by informative simulation results. Also, IGBT inverter with high speed DSP, TI TMS320 F243 is built to provide experimental results.**

I. INTRODUCTION

There is a growing interest in electric vehicle (EV) and hybrid electric vehicle (HEV) due to environmental concerns and they offer the most promising solutions to reduce vehicular emissions, which is the main problem of internal combustion engine (ICE). Since the advancement in battery technology has been relatively sluggish, compared with the power electronics area, the handicap of short range associated with EV still remains. With this technology limitation, the HEV seems to be the viable alternative to the ICE automobile at the present [1]. Hybrid electric vehicles can be classified as series and parallel configurations, as shown in Fig. 1.

In recent, much effort is directed toward developing electric propulsion system of EV and HEV [1]. The electric propulsion system is one of the main parts and requires multi-disciplinary power electronics technologies, including motor, power converter circuitry, power switching device, microprocessor, DSP, and PWM control strategy. And, the recent advancement of power electronics technologies accelerates the research of propulsion system [2]. Although their technical advantages are generally acknowledged, researchers are becoming aware of their cost and are exploring the possibility of cost reduction. The cost reduction of electric propulsion is accomplished by the two approaches. One is the topological approach and the other is control approach. In topology, minimum number of switches is used to compose the power converter circuit. In control approach, algorithms are designed and implemented in conjunction with the reduced parts converter to produce the desired dynamic and static speed and torque characteristics. Moreover, the cost and reliability of the electric propulsion system can be further improved by sensorless method of control [3]-[4]. The sensorless control with high speed DSP, such as TI TMS320F243 can replaces the position sensors and speed encoders, which were customarily mounted on the machine's shaft and were one of the main parts to increase the system cost.

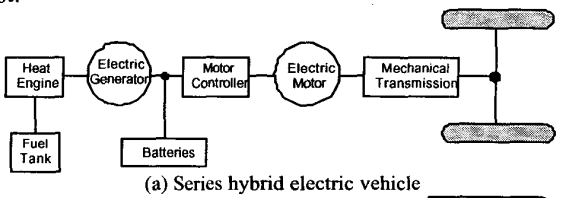

(a) Series hybrid electric vehicle

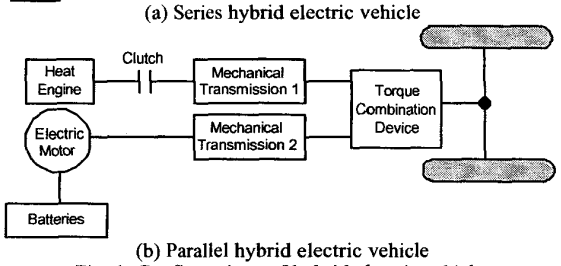

(b) Parallel hybrid electric vehicle

Fig. 1. Configurations of hybrid electric vehicle.

Also, the brushless dc motor (BLDCM) is gaining so much interest as a strong candidate for EV and HEV due to the following reasons over the induction motor [5]-[6]: high power density, lower mass and volume, high torque, high efficiency, easy to control, simple hardware and software, and lower maintenance. Furthermore, it should be noted that the generating control could be easily obtained in the BLDCM, which is very important characteristic in EV and HEV applications. However, until now, the reduced parts converters have mainly been developed in the ac induction motor applications [7]-[9].

Therefore, in this paper, we propose an advanced BLDCM drive, which can be a strong solution for low cost and high performance EV and HEV propulsion system. The proposed system consists of a four-switch converter to drive three-phase BLDCM and a novel PWM control strategy to generate robust speed and torque responses. It is very simple to be implemented from the hardware and software points of view. Therefore, based on the developed PWM control strategy, the four-switch three-phase BLDCM drive could be a good alternative to the conventional six-switch counterpart

The theoretical explanation and analysis of the proposed system are explained in detail. The performance is analyzed

0-7803-7091-0/01/$10©2001 IEEE

by comparison to the conventional six-switch three-phase BLDCM drive. Also, simulation and experimental results are provided to verify the validity of the proposed low cost BLDM drive.

II. ADVANCED BLDCM DRIVE FOR ELECTRIC PROPULSION SYSTEM

Figure 2 shows the electric propulsion system in EV and HEV. In the propulsion system, PWM converter is conventionally composed of six-switch converter configuration to drive three-phase BLDCM, as shown in Fig. 3. Our team at Texas A&M has been investigating the possibility of the reduced converter for BLDCM drive. As a result, we found that one switch leg (two switches) in the conventional six-switch converter is redundant to drive the three-phase BLDCM. It results in the possibility of the four-switch configuration instead of the six switches, as shown in Fig. 4. However, in the four-switch converter, generating of 120° conducting current profiles is inherently difficult due to its limited voltage vectors, as shown in Fig. 5. Therefore, a new control scheme should be developed to drive this converter properly. The solutions can be obtained from modification of the conventional voltage controlled PWM strategies, such as the space vector PWM (SVPWM). However, the voltage controlled based approaches could become too much complicated, so that it is hard to be regarded as optimal control strategies for the four-switch BLDCM drive.

In this paper, we propose a novel PWM control technique based on the current controlled PWM method, instead of the voltage controlled PWM, which will be called the direct current controlled PWM. The developed direct current controlled PWM method generates robust speed and torque responses and is very simple to be implemented from the hardware and software points of view.

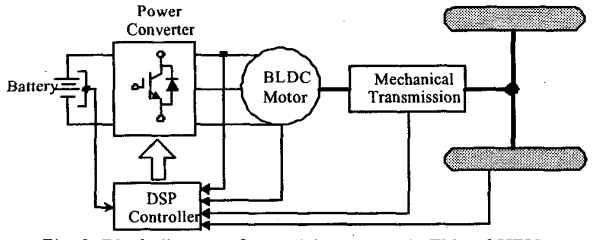

Fig. 2. Block diagram of propulsion system in EV and HEV.

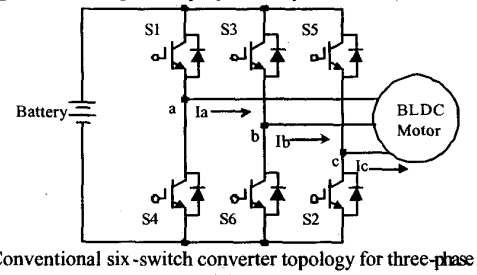

Fig. 3. Conventional six-switch converter topology for three-phase BLDCM in propulsion system.

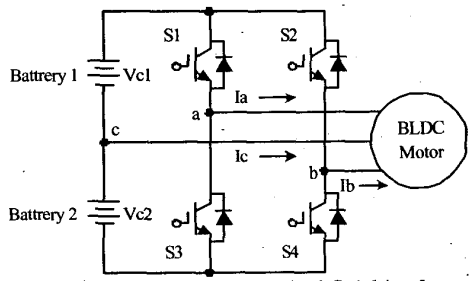

Fig. 4. Proposed four-switch three-phase BLDCM drive for propulsion system in EV and HEV.

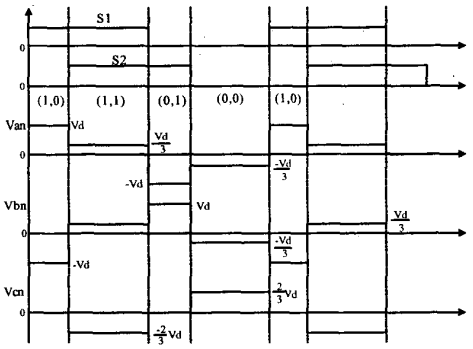

Fig. 5. Inherent problem of the four-switch converter to generate 120° conduction.

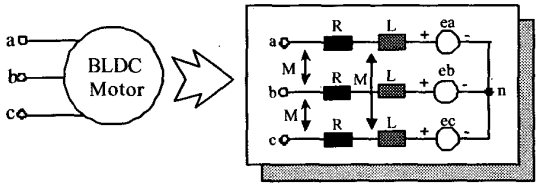

BLDC Motor Model

(a) Representation of the three-phase BLDC motor

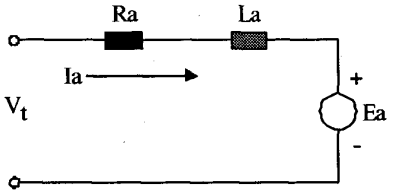

(b) Equivalent circuit of the BLDC motor

Fig. 6. Equivalent model of the BLDC motor.

III. ANALYSIS OF THREE-PHASE BLDC MOTOR DRIVE

The analysis is based on the following assumption and the BLDC motor model of Fig. 6(a) for simplification:

1) The motor is not saturated.
2) Stator resistances of all the windings are equal and self and mutual inductances are constant.
3) Power semiconductor devices in the inverter are ideal.
4) Iron losses are negligible.

Under the above assumptions, a BLDC motor can be represented as

$$\begin{bmatrix} v_a \\ v_b \\ v_c \end{bmatrix} = \begin{bmatrix} R & 0 & 0 \\ 0 & R & 0 \\ 0 & 0 & R \end{bmatrix} \begin{bmatrix} i_a \\ i_b \\ i_c \end{bmatrix} + \begin{bmatrix} L-M & 0 & 0 \\ 0 & L-M & 0 \\ 0 & 0 & L-M \end{bmatrix} \frac{d}{dt} \begin{bmatrix} i_a \\ i_b \\ i_c \end{bmatrix} + \begin{bmatrix} e_a \\ e_b \\ e_c \end{bmatrix} \quad (1)$$

where e_a, e_b, and e_c are trapezoidal shaped back EMFs. The electromagnetic torque is expressed as

$$T_e = \frac{1}{\omega_r}(e_a i_a + e_b i_b + e_c i_c) \quad (2)$$

And, the interaction of T_e with the load torque determines how the motor speed builds up:

$$T_e = T_L + J\frac{d\omega_r}{dt} + B\omega_r \quad (3)$$

where T_L is load torque, J is inertia, and B is damping.

Based on the equivalent circuit of Fig. 6(c), the system equations can be expressed by using Laplace transform [10] as

$$\begin{aligned} V_t(s) &= E_a(s) + (R_a + sL_a)I_a(s) \\ E_a(s) &= k_E \omega_r(s) \\ T_e(s) &= k_T I_a(s) \\ T_e(s) &= T_L(s) + (B + sJ)\omega_r(s) \end{aligned} \quad (4)$$

From (4), superposition principle yields

$$\begin{aligned} \omega_r(s) = &\frac{k_T}{(R_a + sL_a)(sJ + B) + k_T k_E} V_t(s) \\ &- \frac{R_a + sL_a}{(R_a + sL_a)(sJ + B) + k_T k_E} T_L(s) \end{aligned} \quad (5)$$

Considering $B = 0$, (5) results in closed-loop transfer function as

$$\begin{aligned} G(s) = \left.\frac{\omega_r(s)}{V_t(s)}\right|_{T_L(s)=0} &= \frac{k_T}{(R_a + sL_a)(sJ + B) + k_T k_E} \\ &= \frac{k_T}{sJ(R_a + sL_a) + k_T k_E} \\ &= \frac{1}{k_E\left(s^2 \frac{L_a J}{k_T k_E} + s\frac{R_a J}{k_T k_E} + 1\right)} \end{aligned} \quad (6)$$

From (6), mechanical time constant (τ_m) and electrical time constant (τ_e) are defined as

$$\tau_m = \frac{R_a J}{k_T k_E}, \quad \tau_e = \frac{L_a}{R_a} \quad (7)$$

Using the time constants, (6) is expressed as

$$\begin{aligned} G(s) = \left.\frac{\omega_r(s)}{V_t(s)}\right|_{T_L(s)=0} &= \frac{1}{k_E(s^2\tau_m\tau_e + s\tau_m + 1)} \\ &= \frac{1}{k_E(s\tau_m + 1)(s\tau_e + 1)} \quad (\because \tau_m \geq \tau_e) \end{aligned} \quad (8)$$

IV. FOUR-SWITCH THREE-PHASE BLDC MOTOR DRIVE

A. Operational Principle of Direct Current Controlled PWM

As shown in Fig. 4, the developed four-switch three-phase BLDC motor drive is consisted of two switch legs (S_1, S_2, S_3, S_4) and split capacitor bank. Two phases of the motor are connected to the switch legs and the other phase is connected to the midpoint of DC-Link capacitors. Topologically, the four-switch converter is identical to the case of induction motor drive. However, as explained earlier, it is inherently impossible to generate the 120° conducting three-phase current profiles. Therefore, a new and optimal PWM control strategy should be developed to control the three-phase currents to take a form of quasisquare waveform in order to synchronize with the trapezoidal back EMF to produce the constant and maximum torque.

From the motor point of view, even though the BLDC motor is supplied by the four-switch converter, ideal back EMF of three-phase BLDC motor and the desired current profiles can be described as shown in Fig. 7. From the detailed investigation of the four-switch configuration and back EMF and current profiles, we could come up with a PWM control strategy for the four-switch three-phase BLDC motor drives as follows: Under the balanced condition, the three-phase currents always meet the following condition, such as

$$I_a + I_b + I_c = 0 \quad (9)$$

Then, (9) can be modified as

$$I_c = -(I_a + I_b) \quad (10)$$

Equation (10) implies that one of the three-phase currents can be composed by the summation of the other phases. It means that control of the two-phase currents can guarantee the generation of the 120° conducting three-phase currents profiles. For completing this task, the two-phase currents are directly controlled using the hysteresis current control method by four switches, so that it is called as direct current controlled PWM scheme. Based on the direct current controlled PWM, the four-switch three-phase BLDC motor drive can be divided into six operating modes and the switching sequences are determined according to the operating modes. The detailed switching conduction status is depicted in Figs. 7 and 8.

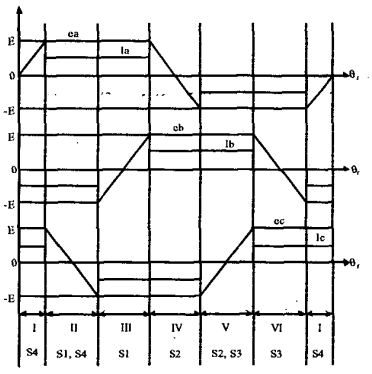

Fig. 7. Back EMF and current profiles of the four-switch converter.

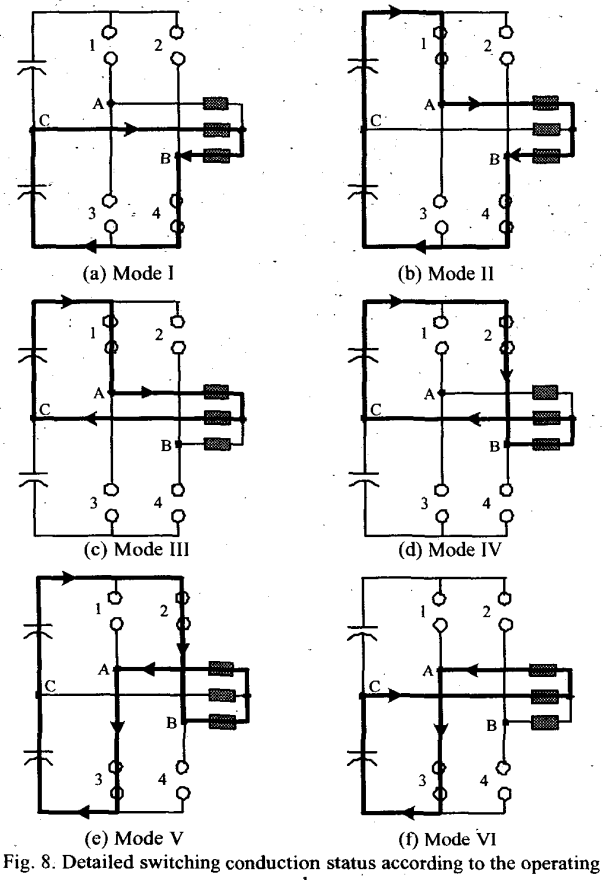

Fig. 8. Detailed switching conduction status according to the operating modes.

B. Implementation of the Direct Current Controlled PWM

As an example of the phase A, the direct current control mechanism can be more clearly visualized with the help of Fig. 9.

(1) Case I: $I_a > 0$

- Period 1: $I_a < Lower\ Limit(LL) \rightarrow$ Switch S_1 is turned on.
- Period 2: $I_a > Upper\ Limit(UL) \rightarrow$ Switch S_1 is turned off and D_3 is conducted.
- Period 3: $LL < Ia < UL$ *and* $dI_a / dt > 0 \rightarrow$ S_1 is turned on.
- Period 4: $LL < Ia < UL$ *and* $dI_a / dt < 0 \rightarrow$ S_1 is turned off and D_3 is conducted.

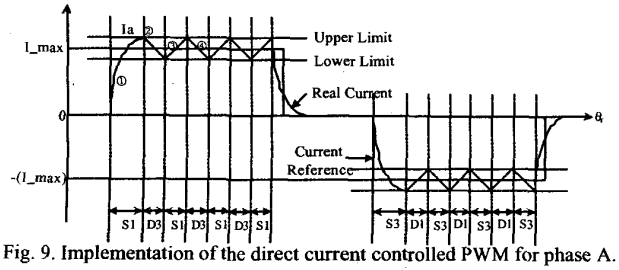

Fig. 9. Implementation of the direct current controlled PWM for phase A.

(2) Case II: $I_a < 0$

- Period 1: $I_a > UL \rightarrow$ Switch S_3 is turned on.
- Period 2: $I_a < LL \rightarrow$ Switch S_3 is turned off and D_1 is conducted.
- Period 3: $LL < Ia < UL$ *and* $dI_a / dt < 0 \rightarrow$ S_3 is turned on.
- Period 4: $LL < Ia < UL$ *and* $dI_a / dt > 0 \rightarrow$ S_3 is turned off and D_1 is conducted.

The same explanation can be applied to the control of the phase B. Also, the voltage and current equations for each mode can be expressed as

- Mode I: $V_{c2} = 2RI_c + 2L\frac{dI_c}{dt} + e_{cb}$
- Mode II: $V_{c1} + V_{c2} = 2RI_a + 2L\frac{dI_a}{dt} + e_{ab}$
- Mode III: $V_{c1} = 2RI_a + 2L\frac{dI_a}{dt} + e_{ac}$
- Mode IV: $-V_{c2} = 2RI_b + 2L\frac{dI_b}{dt} + e_{bc}$
- Mode V: $-(V_{c1} + V_{c2}) = 2RI_b + 2L\frac{dI_b}{dt} + e_{ba}$
- Mode VI: $-V_{c1} = 2RI_c + 2L\frac{dI_c}{dt} + e_{ca}$

C. Back EMF Compensation Problem

Special attention should be paid to the Mode II and Mode V. In these modes, the phases A and B are conducting current and the phase C is regarded as a silent phase, so that it is expected that there is no current in the phase C. However, the back EMF of phase C can act as a current source and causes the additional and unexpected current, resulting in current distortion in the phase A and B. Therefore, in the direct current controlled PWM, the back EMF compensation problem should be considered. This phenomenon can be explained with the simplified equivalent circuit in Fig. 10. As an example of Mode II, if the phase A current is controlled and determines the switching signals of S_1 and S_4, the phase A current can be regarded as a constant current source. In this case, the phase B current can be distorted by the phase C current. On the other hand, if the phase B is controlled, the phase B current can be a constant current source, and then the phase A current can be distorted. The same explanation can be applied to Mode V. From the equivalent circuits of Fig. 10, one can come up with a solution. If the phase A and B are regarded as independent current source, the back EMF of phase C cannot act as a current source, so that there is no current in the phase C. It means that in the direct current controlled PWM, the phase A and phase B currents should be controlled independently and the switching signals of S_1 (S_3) and S_4 (S_2) should be determined independently. The back EMF compensation problem will be examined and explained in detail with the experimental results in the Section V.

The dynamic control of the developed system is established by the speed/torque control loop in cooperation with rotor position sensor and direct current controller as shown in Fig. 11.

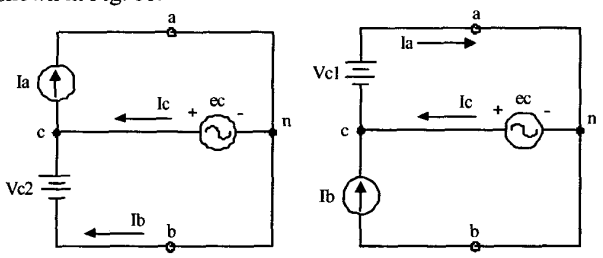

Fig. 10. Simplified equivalent circuit of Mode II to explain the back EMF compensation problem. (a) Case of phase A is controlled. (b) Case of phase B is controlled.

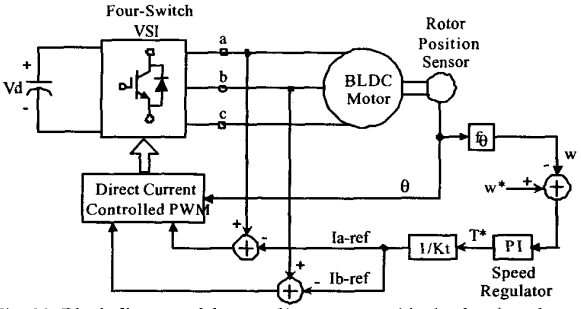

Fig. 11. Block diagram of the speed/torque control in the developed system.

V. SIMULATION AND EXPERIMENATL RESULTS

Table I shows the BLDC motor specification to examine the performance of the developed four-switch three-phase BLDC motor system. Figs. 12 and 13 show the simulation results of the conventional six-switch converter and the developed four-switch converter using direct current controlled PWM method, respectively. As shown in Fig. 13, the actual 120° conducting three-phase currents are successfully obtained in the four-switch converter.

In order to carry out the experimental verification, a BLDC motor drive test-bed is built using PowerRex IGBTs Module as a main switches to compose the converter circuit, Fuji EXB-841 as a gate driver, TI TMS320C F243 as a controller, hall sensor as a position feedback sensor, and 1HP permanent magnet DC motor as a constant torque load. Fig. 14 shows the actual back EMF waveforms, which are measured from the BLDC motor in the test bed. The experimental current waveforms of the conventional six-switch three-phase BLDC motor drive are shown in Fig. 15, using the hysteresis current control with 160VDC DC-Link voltage. The performance of the developed four-switch three-phase BLDC motor drive system with the direct current controlled PWM strategy is examined in Figs. 16 and 17. Fig. 16 shows the back EMF compensation problem, which was explained in Section IV. From Fig. 16, it is clearly noted that when the phase A current is controlled, the phase B current is distorted by the back EMF of phase C and when the phase B is measured and controlled to generate the gating signals of S_2 and S_3, the phase A current is out of control, so that it becomes distorted. On the other hand, when the phase A and B are controlled independently, one can obtain the proper current profiles as shown in Fig. 17(a). The detailed switching signal waveforms can be observed from Fig. 17(b). As shown in Fig. 17(b), it is noted that the switching signals of S_1 and S_4 are not identical. It means that the phase A and B currents are controlled independently to prevent the effect of back EMF of phase C during Modes II and V. From the simulation and experimental results, the validity of the developed four-switch three-phase BLDC motor drive using the direct current controlled PWM is successfully verified.

Table I Motor Specification (LL: line-to-line)

K_t	1.605[Nm]	R_{LL}	7.82[Ω]
K_{e_LL}	1.146[V/(rad/sec)]	$(L\text{-}M)_{LL}$	77.6[mH]
No. of Pole	4[Pole]	Power	1[HP]

VI. CONCLUSIONS

Through our study of old and new concepts of the reduced parts converter topologies and their control strategies, we have developed several types of low cost power converter system. Furthermore, we are developing a better concept at the present for IM, PMSM, SynRM, and BLDCM. We can develop these for EV and HEV applications or adapt a variation of our drives to their particular needs. Moreover, new sensorless control strategies can be directly combined into our several low cost converter topologies, which will be explained in future papers. Consequently, sensorless BLDCM drive without limitation of speed range is ready to be commercialized.

REFERENCES

[1] M. Ehsani, K. M. Rahman, and H. A. Toliyat, "Propulsion system design of electric an hybrid vehicles," *IEEE Transactions on Industrial Electronics*, vol. 44, no. 1, pp. 19-27, February 1997.

[2] C. C. Chan and K. T. Chau, "An overview of power electronics in electric vehicles," *IEEE Transactions on Industrial Electronics*, vol. 44, no. 1, pp. 3-13, February 1997.

[3] J. P. Johnson and M. Ehsani, "Review of sensorless methods for brushless dc," *IEEE-IAS'99 Conference*, pp. 143-150, October 1999.

[4] J. P. Johnson and M. Ehsani, "Sensorless brushless dc control using a current waveform anomaly", *IEEE-IAS'99 Conference*, pp. 151-158, October 1999.

[5] M. Umeda, S. Hashimoto, J. Tsujimura, H. Itoh, M. Hirata, and S. Kato, "Permanent magnet motor for EV," *IEEE Power Electronics and Drive Systems Conference*, pp. 792-796, 1995.

[6] N. Schofield and M. K. Jenkins, "High performance brushless permanent magnet traction drives for hybrid electric vehicles," *IEE Colloquium on Machines and Drives for Electric and Hybrid Vehicles*, pp. 4/1-4/6, 1996.

[7] H. W. Van Der Broeck and J D. Van Wyk, "A comparative investigation of a three-phase induction machine drive with a component minimized voltage-fed inverter under different control options," *IEEE Transactions on Industry Applications*, vol. 20, no. 2, pp. 309-320, Mar./Apr. 1984.

[8] H. W. Van Der Broeck and H. C. Skudelny, "Analytical analysis of the harmonic effects of a pwm ac drive," *IEEE Transactions on Power Electronics*, vol. 3, no. 2, pp. 216-223, Apr. 1988.

[9] F. Blaabjerg, D. O. Neacsu, and J. K. Pedersen, "Adaptive SVM to compensate dc-link voltage ripple for four-switch three-phase voltage-source inverter," *IEEE Transactions on Power Electronics*, vol. 14, no. 4, pp. 743-752, July 1999.

[10] N. Mohan, T. M. Undeland, and W. P. Robbins, *Power Electronics: Converters, Applications, and Design*, New York: Wiley, 1995.

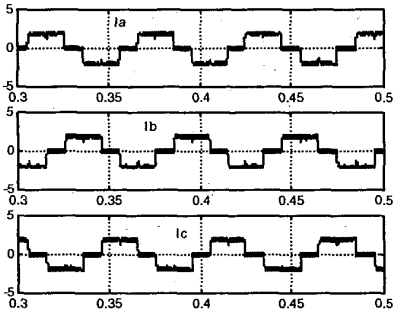

Fig. 12. Simulation phase current waveforms in the conventional six-switch three-phase BLDC motor drive (speed: 1000[rpm]).

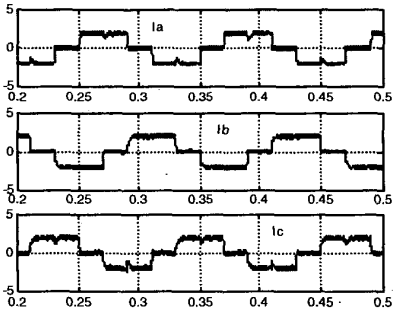

Fig. 13. Simulation phase current waveforms in the developed four-switch three-phase BLDC motor drive using direct current controlled PWM.

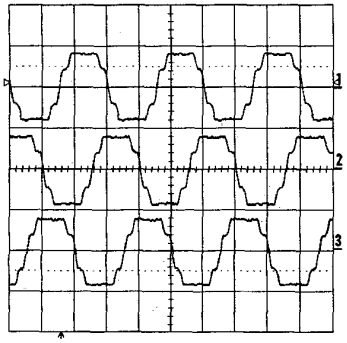

Fig. 14. Back-EMF waveforms (50V/div., 20ms/div.).

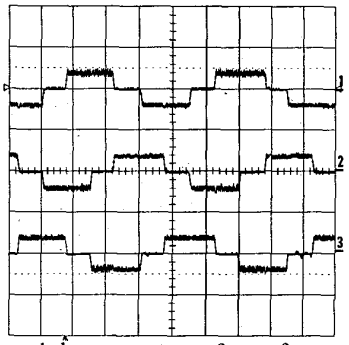

Fig. 15. Experimental phase current waveforms of conventional six-switch three-phase BLDC motor drive (top to bottom: I_a, I_b, I_c; 20ms/div., 5A/div.).

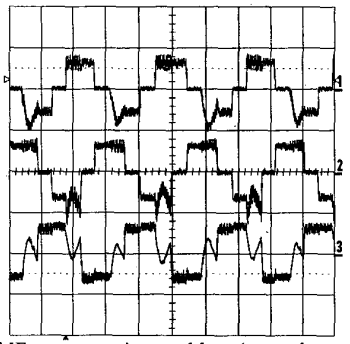

Fig. 16.Back EMF compensation problem (top to bottom: I_a, I_b, and I_c; 50ms/div., 2A/div.).

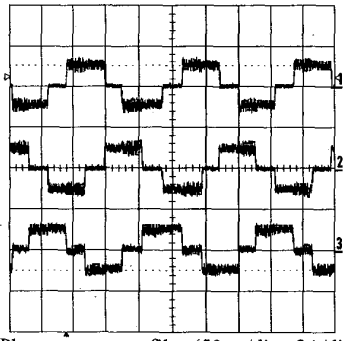

(a) Phase current profiles (50ms/div., 2A/div.).

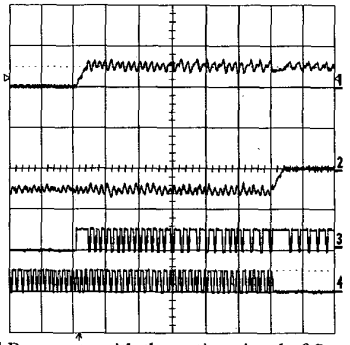

(b) Phase A and B currents with the gating signal of S_1 and S_4 (5ms/div., 2A/div., 10V/div.).

Fig. 17. Experimental voltage and current waveforms of the developed four-switch three-phase BLDC motor drive.